Particle-in-cell method for plasmas in the one-dimensional electrostatic limit

Article *in* American Journal of Physics · March 2023

DOI: 10.1119/5.0135515

3 authors, including:

J. A. Valdivia
University of Chile
232 PUBLICATIONS **4,233** CITATIONS

MARCH 01 2023

Particle-in-cell method for plasmas in the one-dimensional electrostatic limit

Sara Gomez ; Jaime Humberto Hoyos; Juan Alejandro Valdivia

American Journal of Physics 91, 225–234 (2023)
https://doi.org/10.1119/5.0135515

COMPUTATIONAL PHYSICS

The Computational Physics Section publishes articles that help students and instructors learn about the computational tools used in contemporary research. Interested authors are encouraged to send a proposal to the editors of the Section, Jan Tobochnik (jant@kzoo.edu) or Harvey Gould (hgould@clarku.edu). Summarize the physics and the algorithm you wish to discuss and how the material would be accessible to advanced undergraduates or beginning graduate students.

Particle-in-cell method for plasmas in the one-dimensional electrostatic limit

Sara Gomez[a)]
Escuela de Ciencias Aplicadas e Ingeniería, Universidad EAFIT, Medellín, Colombia

Jaime Humberto Hoyos
Facultad de Ciencias Básicas, Universidad de Medellín, Medellín, Colombia

Juan Alejandro Valdivia
Depto. de Física, Facultad de Ciencias, Universidad de Chile, Santiago, Chile

(Received 11 October 2022; accepted 21 November 2022)

We discuss the particle-in-cell (PIC) method, which is one of the most widely used approaches for the kinetic description of plasmas. The positions and velocities of the charged particles take continuous values in phase space, and spatial macroscopic quantities, such as the charge density and self-generated electric fields, are calculated at discrete spatial points of a grid. We discuss the computer implementation of the PIC method for one-dimensional plasmas in the electrostatic regime and discuss a desktop application (PlasmAPP), which includes the implementation of different numerical and interpolation methods and diagnostics in a graphical user interface. To illustrate its functionality, the electron-electron two-stream instability is discussed. Readers can use PlasmAPP to explore advanced numerical methods and simulate different phenomena of interest.

https://doi.org/10.1119/5.0135515

I. INTRODUCTION

The study of plasmas by analytical methods alone is not sufficient.[1,2] In many situations, plasmas can be considered to be collisionless, particularly in space and astrophysical environments, where short-range binary interactions can be neglected.[3] An approach that uses the collisionless approximation is the particle-in-cell (PIC) method, which was proposed in the 1950s and has become widely used due to the great advances in computing power. The method was developed by John Dawson and Oscar Buneman and was first applied to systems of 100–1000 particles.[4] The method was extended by Dawson[5] in 1983. In 1988, Hockney and Eastwood published a highly acclaimed book,[6] and in 1991, Birdsall and Langdon published the most widely recognized book on the method.[1] Both books describe the PIC method and discuss different simulations and analyses.

Simulations are widely used to study different kinds of microinstabilities and waves common in space plasmas such as the electron-electron two-stream instability,[7] Buneman instability,[8] and ion-acoustic waves.[9] There are now open source programs such as Jupyter notebooks for educational plasma simulations[10] and the graphical user interface developed by Omura and Matsumoto.[11]

Reference 12 discusses the implementation of the two-dimensional electrostatic PIC method in detail. Although two dimensions yield a more realistic view of plasmas, the computational cost and the complexity of the simulations are much greater than one dimension. As will be seen in Sec. II, PIC codes are usually built over an Eulerian mesh, and two dimensions usually requires the order of $32 \times 32 = 1024$ grid points, in contrast to one dimension (1D) for which the minimum is the order of 32 grid points, meaning that the computational cost increases dramatically in 2D systems.[1] Moreover, collisionless plasmas contain many particles in a characteristic volume known as the Debye sphere, whose radius is the Debye length λ_D. The number of particles in this volume is $N_D \sim \lambda_D^d$. If a 3D system has $N_D = 10^6$, for example, then $N_D \approx (10^6)^{2/3} = 10^4$ in 2D, and $N_D \approx (10^6)^{1/3} = 10^2$ in 1D, which implies a lower computational effort for the 1D system.[1] Understanding two-dimensional simulations requires a more advanced mastery of the PIC method and of the physics involved, and thus, a one-dimensional system provides a good starting point for students.

Although Refs. 1, 5, 6, and 10–12 explain the PIC method in detail, its understanding requires the mastery of numerical methods and advanced electromagnetic concepts. The main objective of this paper is to explain the PIC method so that students who have taken a course in integral calculus and a basic course in electrostatics can understand the method. In this spirit, we consider the simplest plasma, i.e., a Coulomb plasma, for which the system is free of magnetic fields and the plasma waves contain only electric fields varying in a longitudinal direction. A graphical user interface (PlasmAPP) is developed

to help teachers and students study basic plasma phenomena in an interactive way.

Our numerical implementation of the PIC model is based on the Lapenta open source code[13] for which the plasma is composed of moving electrons and ions fixed in the background. We extended the code to include the motion of ions, two interpolation methods, different numerical methods for the solution of the differential equations, and multiple diagnostics. The numerical methods explained in Sec. III are the direct integration of Gauss's law of electrostatics using the trapezoid method to approximate integrals, Euler's method for the time integration of Newton's second law for particle dynamics, and the nearest grid point as the simplest interpolation method. More advanced numerical methods, which can increase the efficiency and the speed of the simulations, are explained in the supplementary material.[14,15]

To illustrate the application of the one-dimensional PIC method, we discuss simulations of the electron-electron two-stream instability, a well-known phenomenon corresponding to an initial condition where two groups of electrons move in opposite directions. This condition departs from thermal equilibrium characterized by a single Maxwellian distribution function.[16] Reference 12 also studied this phenomenon using a two-dimensional simulation. They simulated two electron beams moving with counter-propagating initial velocities along a single Cartesian direction. The subsequent evolution of the system in search of thermal equilibrium leads to the appearance of electric fields pointing mainly along this Cartesian direction. However, it is sufficient to study this situation with a one-dimensional model as we do in the present work. Our code includes comments to facilitate understanding and is freely available.[14,15] Interested readers are guided to choose parameters that can be used to simulate other plasma phenomena such as the Buneman instability, ion-acoustic waves, and Langmuir waves.

This paper is organized as follows: Sec. II explains the basic ingredients of one-dimensional electrostatic PIC simulations. Section III discusses the PIC method and explains its numerical implementation. Section IV discusses the structure of the graphical user interface. Section V contains the results and analysis of the electron-electron two-stream instability simulations. Section VI discusses our conclusions, and Sec. VII includes some suggested problems for interested readers.

II. THEORETICAL BACKGROUND

Because plasmas are composed of millions of particles, the dynamics of each charge as a function of the self-generated electric forces must be followed to find the temporal evolution of the system. This approach requires finding the force experienced by each particle produced by the remaining particles and solving Newton's second law for all of the charges. For a plasma composed of N particles, $N-1$ forces must be calculated to obtain the force experienced by a single charge. If this process is repeated for each of the N particles, $N(N-1)/2$ forces must be calculated, which requires a high computational cost.[1,2,17] It is, therefore, necessary to use methods that approximate the behavior of the plasma at a lower computational cost. There are two general ways to achieve this task. One is the plasma fluid approach, which studies the evolution of macroscopic or bulk properties such as the density, pressure, mean velocities, and mean energy.[18] This approach is useful for understanding plasma dynamics for phenomena occurring on large spatial and temporal scales, in contrast with the small scales associated with the discrete nature of particles.[19] Microscopic temporal and spatial scales are best modeled by a kinetic approach that considers the discrete nature of particles in constant motion due to the self-consistent electromagnetic fields. Because a detailed kinetic description is not computationally efficient due to the large number of particles, it is necessary to use a reduced but sufficiently detailed model that contains information about the particle velocity distribution function.[6]

A kinetic description of plasmas can be achieved by using the Vlasov equation, which gives the spatio-temporal evolution of the distribution function of a single particle.[20] This function is defined in phase space consisting of the spatial coordinates and particle velocities of the particles.[21] The distribution function gives the probability of finding a particle in a small region of phase space.[16] The Vlasov model corresponds to a mean-field theory that evolves the particles by long-range electromagnetic fields calculated as a statistical average over the ensemble of particles. This model is a good approximation for time scales smaller than the characteristic time of the collisions and for large length scales compared to the average particle separation.[22] If the self-consistent coupling of the Vlasov equation with Maxwell's equations is considered, the set of Vlasov-Maxwell equations is obtained.[23]

An approximate solution of the Vlasov equation can be found by finite differences on an Eulerian mesh. During the evolution, particles occupy only a finite region of phase space.[24] For this reason, the implementation of Vlasov codes requires the implementation of arrays of which only a small part is used at any one time, which implies an inefficient use of memory and processing.[25]

An approach with low computational cost is the PIC method. The system consists of superparticles, which represent the dynamics of many, but not too many, real particles moving in continuous phase space (Lagrangian description). The evolution of the distribution function of each species is obtained from the positions and velocities of these superparticles.

If we fix one particle in the plasma, the other particles will move to reduce the electric potential produced by the fixed particle. The resulting shielded electric potential will decay exponentially with a length scale called the Debye length,[20] which is defined as

$$\lambda_{D,\alpha} = \frac{v_{\mathrm{th},\alpha}}{\omega_{p,\alpha}}, \tag{1}$$

where $\omega_{p,\alpha}^2 = n_\alpha q_\alpha^2/m_\alpha\epsilon_0$ is the plasma frequency, $v_{\mathrm{th},\alpha}^2 = k_B T_\alpha/m_\alpha$ is the thermal velocity, n_α is the number density, q_α is the charge, m_α is the mass, and T_α is the temperature of the particle velocity distribution function for species α. Although the electric potential produced by one particle decays with distance, particles closer to the edge of the Debye sphere of the fixed particle can interact with particles nearby but outside the Debye sphere, producing a collective interaction that can propagate through the plasma. Hence, superparticles can be constructed as finite clouds of particles subject to electrostatic interactions with other superparticles that are far away, but experience a weak interaction when they are close to each other.[5] The behavior of the spatial density is not modeled in regions smaller than the cloud size. In this way, it makes sense to construct the charge density and solve for the electric force from the self-consistent electric

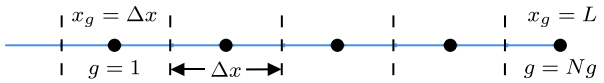

Fig. 1. One-dimensional simulation box of size L. The region between the dashed lines represents the cells of size Δx which are centered at the grid nodes g.

field through Maxwell equations, which are solved on a fixed Eulerian mesh in configuration space.[25] The field can then be interpolated at the position of each superparticle to calculate their acceleration.[26]

III. ELECTROSTATIC ONE-DIMENSIONAL PIC ALGORITHM

In this work, we consider the simplest configuration, which is a one-dimensional system. Many of the technical subtleties of 2D simulations are already present in 1D simulations, both in physics and implementation, so before tackling the task of constructing a simulation for 2D plasmas, it is convenient to understand the difficulties that already appear in 1D plasma simulations. In this type of simulation, harmonic waves with wave propagation vector $\vec{k}$ and frequency ω have their electric field parallel to $\vec{k}$ (parallel propagation). Therefore, if one then wants to advance to electromagnetic or magnetized problems, it is useful to start with 1D and then advance to 2D (oblique propagation).[1] There are a number of current problems in basic and applied research that can be studied with 1D PIC simulations.[27,28]

As mentioned, the PIC method is based on the use of superparticles whose positions and velocities follow a continuous path in phase space, while spatial macroscopic quantities, such as the charge density and self-generated electric field, are calculated at discrete spatial points of a grid (Eulerian description). Figure 1 shows how the Eulerian space grid is created for one dimension. The solid line represents the length of the system ranging from 0 to L. The grid is divided into N_g nodes denoted by discrete indices $g = 1, 2, 3, \ldots, N_g$. The system is periodic, so that the simulation box of length L represents a section of an infinite plasma that repeats periodically in space. For a periodic system, nodes divide the total length L into N_g cells of size Δx, centered on the grid points as shown in Fig. 1. The grid node positions are $x_g = g\Delta x$, and the length of the system is $L = N_g \Delta x$.[6]

Periodic boundary conditions are used so that a spatially variable quantity $G(x)$ has a spatial period L, i.e., $G(x + L) = G(X)$. Thus, the last point of the mesh N_g is the same as the first point $g = 0$ (which in not part of the array, which starts at $g = 1$), and the point $N_g + 1$ is the same point as $g = 1$. If a superparticle moves outside the simulation box, it returns to a position inside the box.[1] The distance between nodes should be smaller than the Debye length, and within each cell there are a large number of superparticles so that we can observe collective effects.

The PIC algorithm is depicted in Fig. 2 and is summarized in the following:

(1) Initialize the distribution function of the superparticles indexed by p belonging to species $\alpha =$ ions or electrons, i.e., assign initial positions and velocities to the superparticles. For simplicity, the superparticles are initially positioned uniformly in space and if desired, a small sinusoidal perturbation is added. The initial velocities are assigned according to a Maxwellian distribution corresponding to a system in thermal equilibrium.[16] The width of the Maxwellian is determined by $v_{\text{th},\alpha}$. The function is centered on the speed v_0, which is determined by the nature of the problem being studied.
(2) Calculate the charge density at the grid points ρ_g. Because the coordinate $x_{p,\alpha}$ of the superparticles takes on

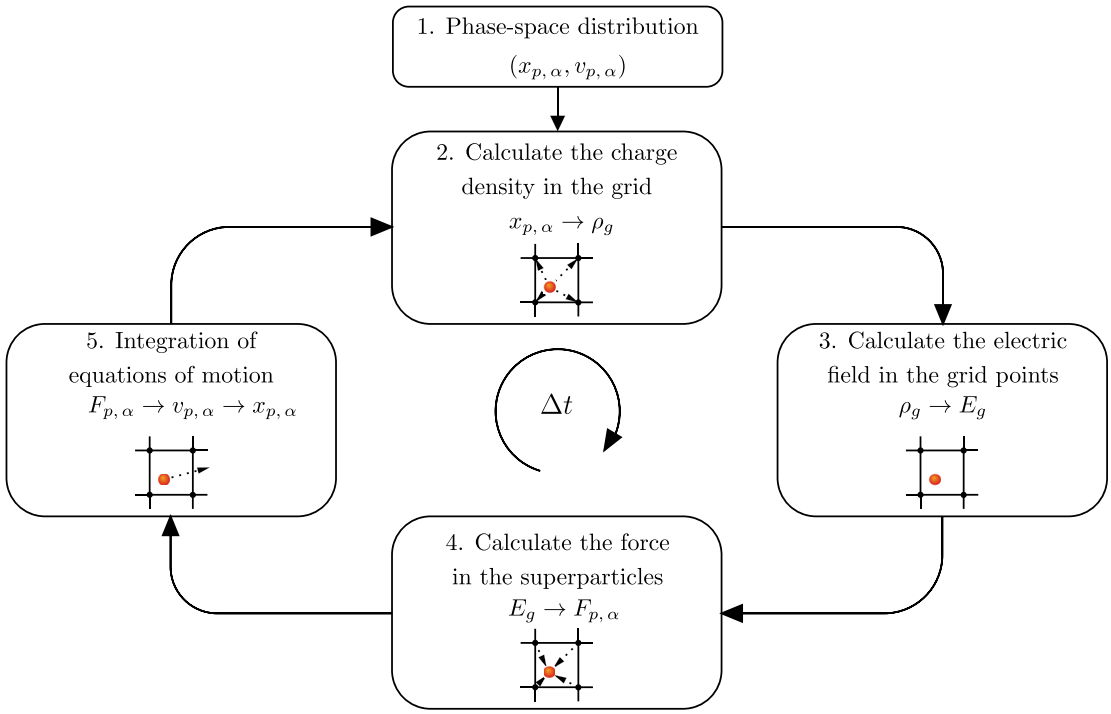

Fig. 2. Electrostatic one-dimensional PIC algorithm. For visualization purposes, the grid shown is two-dimensional. The index p refers to the superparticles, α is the species index, and g is the index of the grid points.

continuous values, it is necessary to determine the contribution of each superparticle to the charge density at the grid points. To do so, we define an interpolation function which determines the weight that each superparticle contributes to the physical properties at the grid points. The simplest method is called the nearest grid point. If the distance between the grid point and the center of superparticle $|x_g - x_{p,\alpha}|$ is less than $\Delta x/2$, a weight of 1 is assigned to that grid point. This method can be expressed using the b-spline flat-top function b_0 as

$$b_0(\chi) = \begin{cases} 1 & |\chi| < 1/2 \\ 0 & \text{otherwise.} \end{cases} \tag{2}$$

The corresponding interpolation function for species α is given by

$$W_\alpha(x_g - x_{p,\alpha}) = b_0\left(\frac{x_g - x_{p,\alpha}}{\Delta x}\right). \tag{3}$$

This interpolation scheme is shown in Fig. 3. In more advanced methods, the superparticle is assigned to more than one grid point.[1,6,15]

(3) The charge density at the grid points g for species α is given by[17]

$$\rho_{g,\alpha} = \frac{q_{p,\alpha}}{\Delta x}\sum_p W_\alpha(x_g - x_{p,\alpha}). \tag{4}$$

The charge of the superparticle is defined as $q_{p,\alpha} = q_\alpha N_{r,\alpha}$, where $N_{r,\alpha}$ is the number of real particles in a superparticle.

(4) The total charge density at grid point g is

$$\rho_g = \sum_\alpha \rho_{g,\alpha}. \tag{5}$$

(5) Given the charge density at the grid points, we calculate the electric field from Poisson's equation at these nodes

$$\frac{d^2\phi(x)}{dx^2} = -\frac{\rho(x)}{\epsilon_0}. \tag{6}$$

If we integrate both sides of Eq. (6) from the left boundary $x = 0$ to an arbitrary point x, we obtain

$$E(x) = E(0) + \frac{1}{\epsilon_0}\int_0^x \rho(x')dx', \tag{7}$$

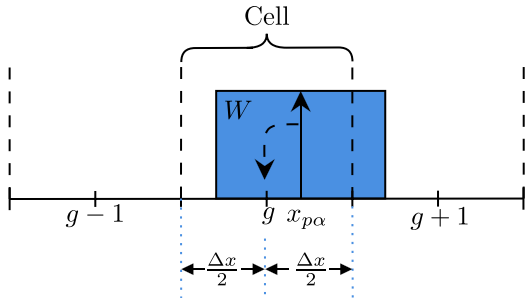

Fig. 3. The nearest grid point interpolation function for superparticle p of species α whose interpolation function with center of mass $x_{p,\alpha}$ contains the grid point g. The curved dashed arrow shows that the entire charge of the superparticle is assigned to g.

where we have used the relation $E(x) = -d\phi(x)/dx$. Note that Eq. (7) requires the value of the electric field at the left boundary $E(0)$. Because of periodic boundary conditions, we also have $E(L) = E(0)$. To obtain an expression for $E(0)$ in terms of the charge density, we integrate Eq. (6) twice and use $\phi(0) = \phi(L)$ to obtain

$$E(0) = -\frac{1}{L}\int_0^L\left(\int_0^{x'}\rho(x'')dx''\right)dx'. \tag{8}$$

Because the charge density is evaluated at the grid points, it is necessary to compute the integrals in Eqs. (7) and (8) using the values of the electric field. For this purpose, the trapezoidal rule is used, so that the electric field at each grid point is given by[29]

$$E_g = E_{g=0} + \frac{\Delta x}{\epsilon_0}\sum_{j=1}^{g-1}\left(\frac{\rho_j + \rho_{j-1}}{2}\right), \tag{9}$$

where $\rho_0 = \rho_{N_g}$. In the same way, it is possible to obtain the electric potential from the relation

$$\phi(x) = \phi(0) - \int_0^x E(y)dy. \tag{10}$$

Because the reference potential $\phi(0)$ in Eq. (10) can be selected arbitrarily, we set $\phi(0) = 0$ for simplicity. We evaluate the integral in Eq. (10) numerically and express ϕ_g as

$$\phi_g = \phi_{g=0} - \Delta x\sum_{j=1}^{g-1}\left(\frac{E_j + E_{j-1}}{2}\right), \tag{11}$$

where $\phi_{g=0} = 0 = \phi_{N_g}$.

(6) To find the electric field $E_{p,\alpha}$ experienced by a superparticle at the continuous position $x_{p,\alpha}$, the nearest grid point method (see Fig. 4) is used so that a superparticle in a cell centered at g (closest grid point to the superparticle) interacts with the electric field E_g. That is, the same interpolation function used in Eq. (3) is applied. Therefore, $E_{p,\alpha}$ is given by

$$E_{p,\alpha} = \sum_g E_g W_\alpha(x_g - x_{p,\alpha}). \tag{12}$$

The same expression can be applied to more general interpolation methods as shown in Refs. 1, 6, 17, and 29. The electric force on the superparticle is

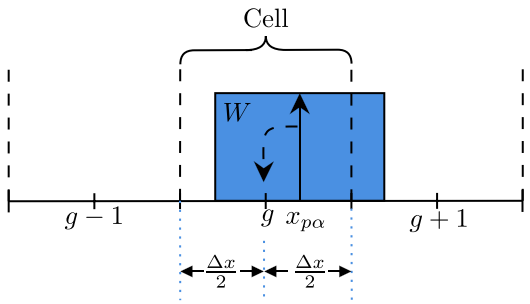

Fig. 4. The nearest grid point interpolation method. The electric field experienced by a superparticle with center of mass at $x_{p,\alpha}$ corresponds to the electric field at node g.

$$F_{p,\alpha} = q_{p,\alpha} E_{p,\alpha}. \tag{13}$$

(7) The dynamics of the center of mass of the superparticles is governed by Newton's equations[6,17]

$$\frac{dx_{p,\alpha}}{dt} = v_{p,\alpha}, \tag{14}$$

$$\frac{dv_{p,\alpha}}{dt} = \frac{F_{p,\alpha}}{m_{p,\alpha}}. \tag{15}$$

The solution of Eqs. (14) and (15) is obtained numerically using the Euler algorithm

$$x_{n+1,p,\alpha} = x_{n,p,\alpha} + v_{n,p,\alpha}\Delta t, \tag{16}$$

$$v_{n+1,p\alpha} = v_{n,p\alpha} + \frac{q_{p,\alpha}}{m_{p,\alpha}} E_{n,p,\alpha}\Delta t, \tag{17}$$

where $t_n = n\Delta t$ and Δt is the time step.

As can be seen in Eq. (17), the acceleration depends on the charge-to-mass ratio of the superparticles. Because the charge and mass of a superparticle p of species α are given by $q_{p,\alpha} = N_{r,\alpha} q_\alpha$ and $m_{p,\alpha} = N_{r,\alpha} m_\alpha$, where $N_{r,\alpha}$ is the number of real particles of species α, we have[25]

$$\frac{q_\alpha}{m_\alpha} = \frac{q_{p,\alpha}}{m_{p,\alpha}}. \tag{18}$$

Hence, the center of mass of a superparticle follows the same trajectory as a real particle because they experience the same acceleration.

IV. PLASMAPP

To make plasma simulations more accessible, we created a program with a graphical user interface which we call PlasmAPP. The program allows users to choose the Euler, leapfrog, or fourth-order Runge-Kutta algorithm for the solution of the equations of motion.[1,29] Users can explore the advantages and disadvantages of these algorithms in terms of numerical stability, speed, and numerical accuracy. The method discussed in Sec. III to find the electric field was the direct integration of Gauss's law. The more advanced possibilities implemented in PlasmAPP include the finite difference method and the fast Fourier transform.[15,29] Users can also select the interpolation method used to assign the charge to the grid and the force calculations. Two possibilities are the nearest grid point explained in Sec. III and the cloud-in-cell method.[1,6,15] PlasmAPP also allows the simulation of phenomena involving ion mobility as well as a fixed neutralizing background. The diagnostics can be chosen and the results can be saved for post-processing. The code can be found at Refs. 14 and 15, and additional information of the code can be found in Ref. 15.

V. RESULTS

We discuss the results of the electron-electron two-stream instability using the Euler method for the equations of motion and direct integration for Gauss's law. The interpolation method used is the nearest grid point. These methods have a greater numerical error than more advanced methods, but they were discussed here because they are easier for students to understand who only have a knowledge of integral calculus and basic electrostatics.

It is convenient to normalize the variables in terms of characteristic times and lengths which define the corresponding scales of interest and avoid the use of very small or very large numbers that lead to numerical errors. By means of an inverse procedure, it is possible to find the physical quantities and their real values. We measured time in terms of the electron plasma period ($\omega_{p,e}^{-1}$), lengths in terms of the Debye length $\lambda_{D,e}$, the mass in terms of the electron mass m_e, and the charge in terms of the proton charge e. The vacuum permittivity ϵ_0 and the Boltzmann constant k_B are set to one. The other units of the physical quantities, such as the velocity, electric potential, electric field, and energy among others, are derived from these fundamental units.

A. Electron-electron two-stream instability

The electron-electron two-stream instability consists of two electron beams with opposite velocities in an immobile ion background. The velocity distribution function is given by[30]

$$f(v_x) = \frac{n_0}{2\sqrt{2\pi}v_{\text{th,e}}} e^{-(v-v_0)^2/2v_{\text{th,e}}^2} + \frac{n_0}{2\sqrt{2\pi}v_{\text{th,e}}} e^{-(v+v_0)^2/2v_{\text{th,e}}^2}.$$

To simulate the electron-electron two-stream instability, we used the parameters $L = 64$, the number of time steps $N_t = 16000$, $\Delta t = 0.1$, the number of grid points $N_g = 256$, the number of electrons of the two beams $N_{e,1} = N_{e,2} = 10000$, the number of ions fixed to the background $N_f = 20000$, $v0_{e,1} = 5$, $v0_{e,2} = -5$, the thermal speed of the two beams $v_{\text{th},e,1} = v_{\text{th},e,2} = 1$, the charge-to-mass relation of the beams $r_{e,1} = r_{e,2} = -1$, and the plasma frequency $\omega_{p,e} = 1$.

The initial state of the system is shown in Fig. 5, where the phase space and the distribution function are displayed. The latter shows the presence of two peaks centered at $v0_{e,1}$ and $v0_{e,2}$, which correspond to five times the thermal speed. These peaks represent the two electron beams. The initial state is charge neutral, and therefore, the electric field in the grid is zero everywhere.

The initial particle velocity distribution function eventually generates an electric field, allowing the beams to interact. Initially, the electric field perturbations are waves that grow exponentially in time, signaling an instability (see Fig. 6).

When the particles interact, they start to form electron phase space holes as observed in Fig. 7, which corresponds to the system at time $t = 350$. As can be seen in Fig. 7(b), the potential reaches a maximum at the center of the electron hole. Because the electric field is equal to the negative derivative of the electric potential, this maximum separates the two regions where the electric field changes sign (see Fig. 7(c)). Because the direction of the electric force is opposite to the direction of the electric field due to the sign of the charge, particles that are to the right (left) of the maximum will experience forces to the left (right), so particles will tend to change their direction of motion, which implies a curvature in phase space that is visualized as a hole (see Fig. 7(a)).[31] Similar results were obtained in two dimensions for simulations of the electron two-stream instability with fixed ions in the presence of a constant external magnetic field.[12]

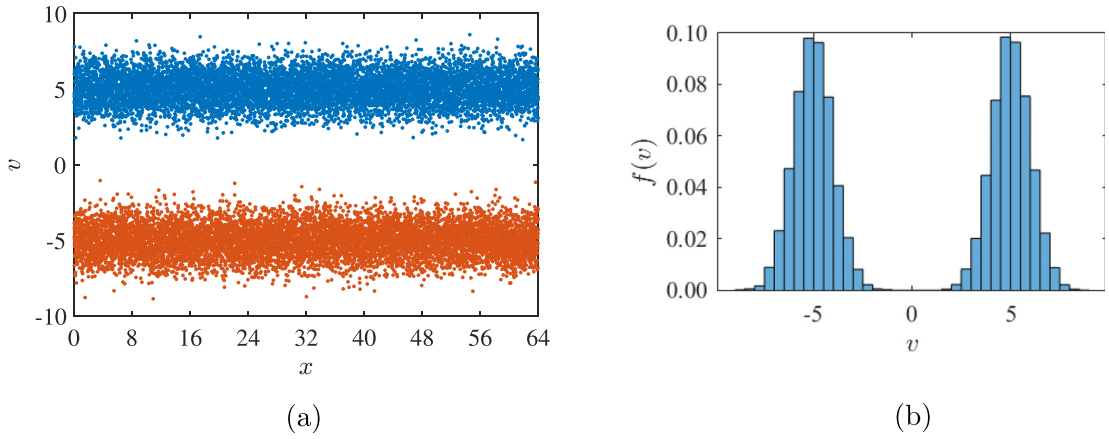

Fig. 5. Initial (a) phase space and (b) velocity distribution function for the electron-electron two-stream instability.

In their simulation, they used the same initial condition as Eq. (19) with the two electron beams moving in opposite directions along the x-direction (see Fig. 5(a) of Ref. 12). They showed that the initial value of the electric potential ϕ is zero, and as the system evolves, waves that vary mainly along the x coordinate begin to appear (see Fig. 6 of Ref. 12) as the system attempts to reach thermal equilibrium. It was also shown that the electric potential is positive at localized regions where electron holes in phase space are formed (see Figs. 5 and 6 of Ref. 12). Because both electron beams in Ref. 12 have initial velocities in just one direction (x), the spatial variation of ϕ through the y coordinate is not significant. Also, the presence of the constant external magnetic field does not influence the evolution in the electrostatic limit because currents are not generated along the x direction according to Ampere's law.[12] Thus, our 1D simulation contains the relevant physics of the instability for this particular initial condition, with the advantage of less computational effort in comparison to the 2D simulations. However, the 2D code implemented in Ref. 12 can be used to simulate the more general oblique propagation.

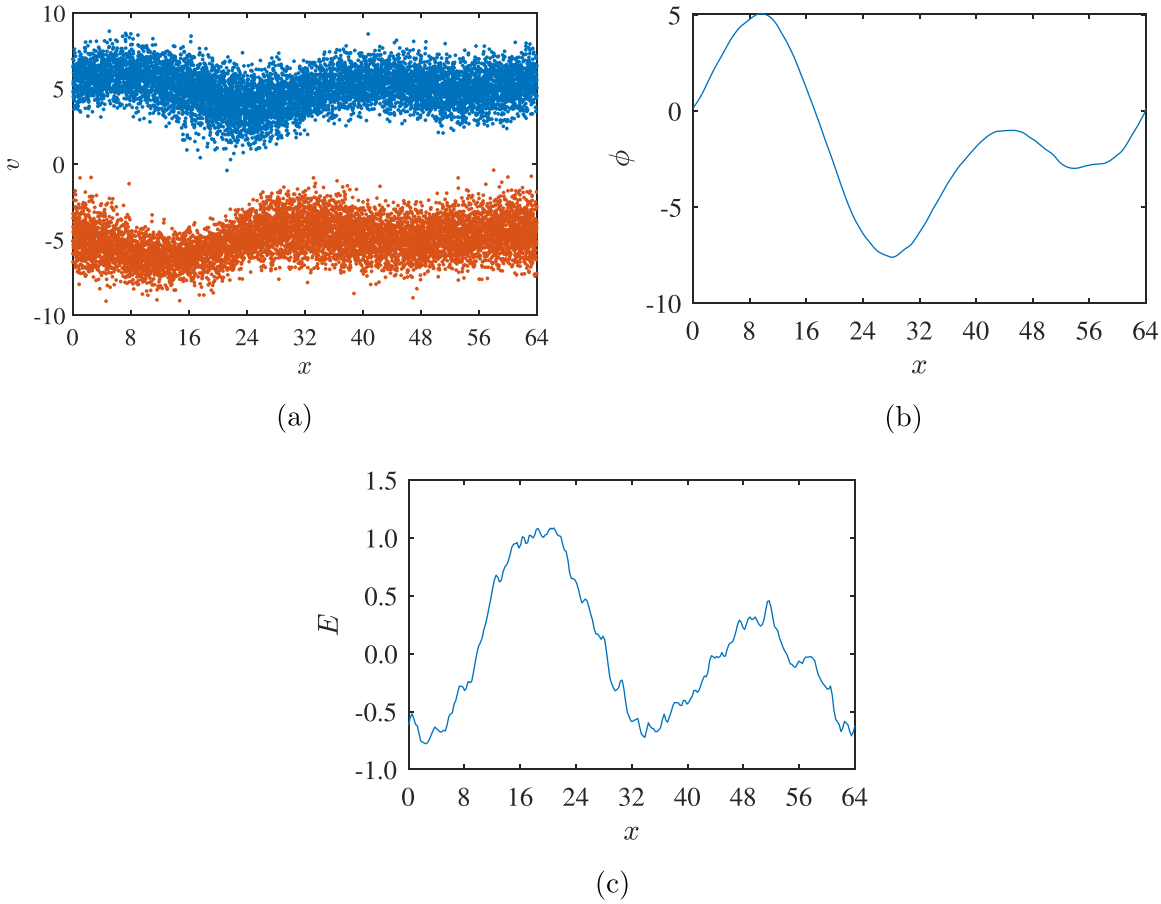

Fig. 6. (a) Phase space; the spatial dependence of (b) the electric potential, and (c) the electric field for the electron-electron the two-stream instability at $t = 10.5$.

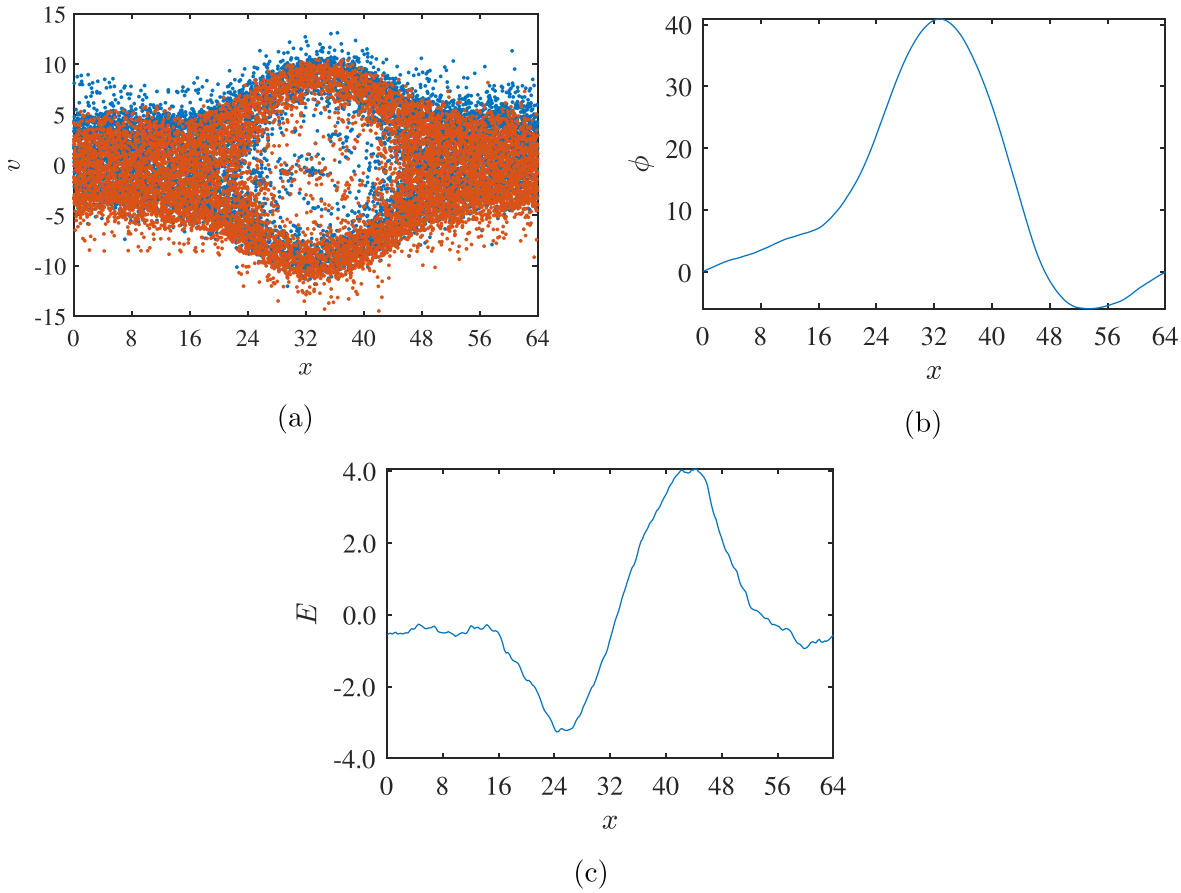

Fig. 7. (a) Phase space, the spatial dependence of the (b) electric potential, and (c) the electric field for the electron-electron two-stream instability at $t = 350$.

Figure 8(a) shows how the energy behaves in the time interval $t = 0$ to $t = 20$. We observe that the kinetic energy ε_k (dashed-dotted line) is much larger than the potential energy ε_p (solid line). When $\varepsilon_k \gg \varepsilon_p$, the system corresponds to a weakly coupled plasma, where long-range interactions dominate over short-range collisions.

The movement of the electron beams with respect to each other causes density perturbations due to the electric force between the particles. These perturbations cause a linear instability characterized by an initial temporal exponential growth of the electric field according to the linear instability theory in plasmas.[1,32,33] This behavior is shown in Fig. 8(a) where the initial growth of the potential energy occurs for $10 \lesssim t \lesssim 14$. At $t = 15.2$, the instability is first saturated and the dynamics becomes nonlinear as shown in Fig. 8(b). After a long time, the beam interaction eventually causes the particles' speeds to converge to the Maxwell-Boltzmann distribution. This long time convergence can be observed using the more advanced methods discussed in Refs. 1, 6, 15, 29, and 34.

The relative percentage error of the total energy at each iteration with respect to the initial total energy was calculated and found to be 0.57%, indicating that the energy is conserved with reasonable accuracy. An analogous error analysis was performed for the total momentum, which

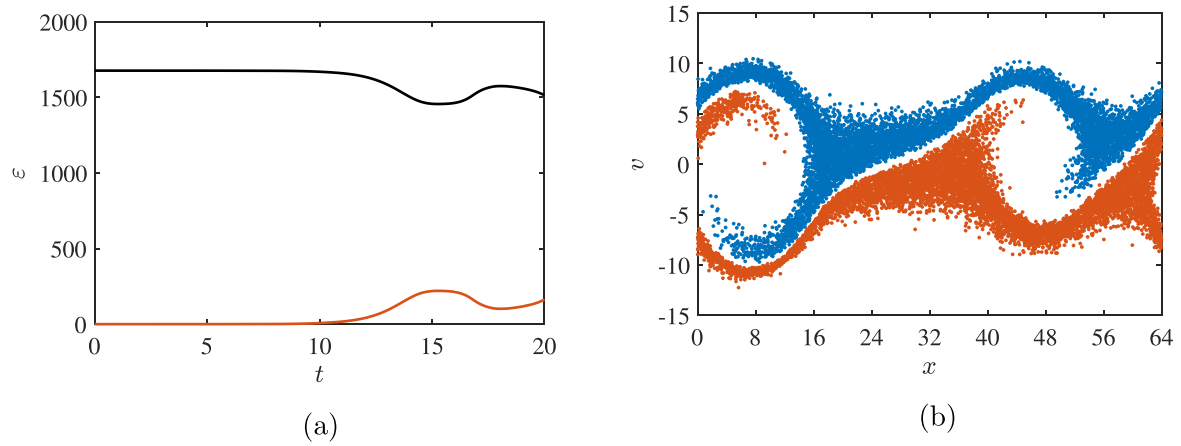

Fig. 8. (a) The time dependence of the kinetic energy ε_k (top curve) and the potential energy ε_p. (b) The phase space at $t = 15.2$, corresponding to the first saturation of the potential energy.

should be zero because the two electron beams have the same density and the same speed but move in opposite directions. The maximum percentage error of the momentum is 5.54×10^{-10} %.

VI. DISCUSSION

To understand the behavior of systems as complex as plasmas, it is helpful to use the simplest possible tools. Visualizing the complex behavior of plasmas provides additional insight, particularly behavior that is not easily accessible by theory.

Plasma evolution involves self-consistent dynamics between the electromagnetic fields and particles, because particles are the source of these fields and particle trajectories are determined by the fields. We have discussed the particle-in-cell method using direct and simple numerical methods and focused on the implementation of a simplified plasma system in the electrostatic regime with a one-dimensional geometry where all physical quantities vary along a single direction.

As an example of the particle-in-cell method and the PlasmAPP program, we simulated the instability of two electron streams where the formation of electron holes in phase space is observed, leading to the generation of bipolar pulses of the electric field, which is consistent with measurements in astrophysical environments.[35] Similar behavior is obtained in one and two dimensions if the initial condition corresponds to electron beams moving along a single Cartesian coordinate. This example shows that the behavior of a system can be simulated by a simpler one-dimensional simulation without the need to introduce the complexities of a simulation in higher dimensions.

Readers can download PlasmAPP from Refs. 14 and 15 and perform simulations of other phenomena of interest, including ion motion, and explore other numerical methods. We hope that we have provided a guide for readers beginning the study of plasma physics and kinetic simulations.

VII. SUGGESTED PROBLEMS

Problem1: Write your own code. We present a brief guide to writing your own electrostatic one-dimensional code using the Euler method for integrating the motion of the particles and direct integration with the trapezoidal rule for determining the electric field. The following steps are for an electron beam with a fixed ion background:

- Define the parameters of the system: Length of the system L, the number of grid points N_g, the cell size Δx, the number of time steps N_t, and the time step Δt. Then define the parameters for the superparticles: The number of superparticles for electrons N_e, the electron plasma frequency $\omega_{p,e}$, the initial velocity $v0_e$, the thermal velocity $v_{\text{th},e}$, and the charge-to-mass ratio r_e. The charge of the superparticle is given by $Q_e = \omega_{p,e}^2/[r_e(N_e/L)]$. To obtain quasi-neutrality of the plasma, a background charge density ρ_{back} must be added $(N_e/L)Q_e + \rho_{\text{back}} = 0$, so that $\rho_{\text{back}} = -(N_e/L)Q_e$.
- Place the particles equally spaced in position. One way to obtain a Maxwellian distribution for the velocities is to multiply the thermal velocity by a function that creates normally distributed random numbers[36,37] and then add the initial velocity of the electrons.
- Apply the interpolation function of Eq. (3) to construct the charge density at the grid points. Include periodic boundary conditions for x_g, which is the position of the grid point closest to the superparticle. Thus, if a superparticle is near $g = 0$, the charge assignment is to the last grid point.
- Calculate the charge density using Eq. (4), including the background density ρ_{back}.
- Use direct integration with the trapezoid rule to compute the electric field at the grid points with Eq. (9).
- To obtain the electric field $E_{p,\alpha}$ experienced by a superparticle at its current position $x_{p,\alpha}$, use Eq. (12) to interpolate this value from the electric fields E_g at the grid points.
- Calculate the new velocities of the superparticles using Eq. (17).
- Use Eq. (16) to calculate the new particle positions. Make sure that you use periodic boundary conditions on the updated positions.

In the following problems, use your own program or the one provided in Refs. 14 and 15 to simulate the evolution of the plasma.

Problem2: Langmuir waves. We can observe Langmuir waves in a plasma in thermal equilibrium. Use the parameters $L = 1024$, $N_t = 8000$, $\Delta t = 0.05$, $N_g = 8192$, $N_e = 50000$, $v_{\text{th},e} = 1$, $r_e = -1$, $\omega_{p,e} = 1$, and set the other parameters to zero. It is necessary in PlasmAPP to define the number of ions in the background to be equal to the number of electrons. The dispersion relation for Langmuir waves is[38]

$$\omega^2 = \pm\omega_{p,e}^2\left(1 + \frac{3}{2}k^2\lambda_{D,e}^2\right), \tag{19}$$

where ω corresponds to the frequency associated with the propagating harmonic fields and k is the corresponding wavenumber. Use your results to plot the theoretical dispersion relation and the simulated one, and determine how they compare. To do so, apply a fast Fourier transform in space and time to the electric field. You should obtain a plot like the one in Fig. 9.

Vary the thermal velocity and observe how the dispersion relation changes. If the thermal velocity becomes smaller, you will obtain cold plasma waves with a frequency equal to

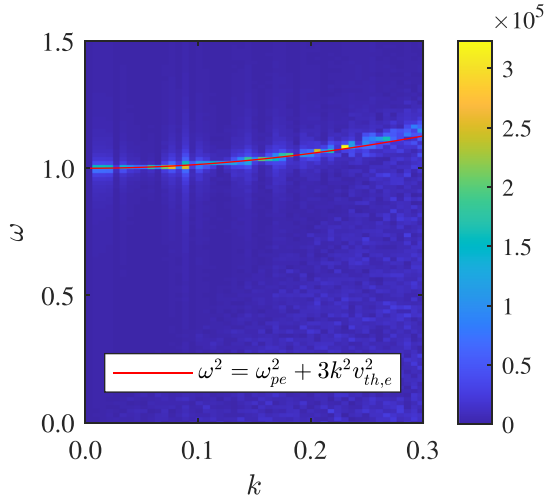

Fig. 9. Ratio of the theoretical to the simulated dispersion relation for Langmuir waves (see problem 2).

$\omega_{p,e}$. You will also see that the numerical error increases because of the non-compliance of the stability conditions.[6] It is important to be aware of the limitations of the program. Add an initial velocity to the beam of electrons, and observe if there is a change in the dispersion relation.

Problem3: Ion-acoustic and Langmuir waves. In problem 2, the ions were fixed. What happens when they are mobile? Add a second species to your program and use the parameters: $L = 2048$, $N_t = 8000$, $\Delta t = 0.05$, $N_g = 8192$, $N_e = 8000$, $N_i = 8000$, $v0_e = 0$, $v0_i = 0$, $v_{\mathrm{th},e} = 10$, $v_{\mathrm{th},i} = 0$, $r_e = -1$, and $r_i = 0.01$. The thermal velocity is increased for ease of visualization. Plot the simulated dispersion relation. You should see another branch corresponding to the dispersion relation of waves generated by the ions. Because they are more massive than electrons, their frequency will be lower. These waves are called ion-acoustic waves, and the dispersion relation is given by[32]

$$\omega^2 = \frac{\omega_{p,i}^2}{1 + (\omega_{p,e}/k^2 v_{\mathrm{th,e}}^2)}. \tag{20}$$

Plot the theoretical dispersion relations of Eqs. (19) and (20) and compare them with your simulations. Then decrease the thermal velocity of the electrons and determine how the dispersion relation changes.

Problem4: Buneman Instability. What happens if there is a relative velocity between two beams of different species? As in the electron-electron two stream instability, an instability, known as the Buneman instability, will be generated. It occurs if the drift velocity between the electron beam and the ions exceeds the thermal velocity of both species.[39] Use the parameters $L = 2\pi$, $N_t = 5000$, $\Delta t = 0.1$, $N_g = 512$, $N_e = 10000$, $N_i = 10000$, $v0_e = 1$, $v0_i = 0$, $v_{\mathrm{th},e} = 0.004$, $v_{\mathrm{th},i} = 0$, $r_e = -1$, $r_i = 0.001$. Plot the phase space, and the spatial dependence of the electric potential and electric field. Observe the time evolution and see how the plasma tries to approach thermal equilibrium. You should first observe the formation of electron phase-space holes with the characteristic bipolar waves of the electric field propagating slower than in the electron-electron two-stream instability.[40] You should also observe how the electron velocity approximates a Maxwell–Boltzmann distribution with a mean velocity approximately equal to the velocity of the ion beam. This system requires a long time to reach thermal equilibrium.

Next increase the charge-to-mass ratio of the ions. What happens to the ion distribution compared to the first simulation? What would happen if instead of ions, you consider a positron beam ($r_i = 1$)?.

ACKNOWLEDGMENTS

S.G. is grateful to Universidad EAFIT for its support. J.H.H. thanks the support of University of Medellin, Colombia and Professor Jaime Araneda of University of Concepción, Chile for his guidance in the first steps of Particle simulations in Plasmas. J.A.V. thanks the support of ANID-Fondecyt under Grant No. 1190703.

AUTHOR DECLARATIONS

Conflict of Interest

The authors have no conflicts to disclose.

[a]ORCID: 0000-0003-1601-6704.

[1]C. K. Birdsall and A. B. Langdon, *Plasma Physics via Computer Simulation* (Taylor and Francis, New York, 2005).
[2]P. L. Pritchett, "Particle-in-cell simulation of plasmas—A tutorial," in *Space Plasma Simulation*, edited by J. Büchner, M. Scholer, and C. T. Dum (Springer Berlin Heidelberg, Berlin, Heidelberg, 2003), pp. 1–24.
[3]R. Treumann and W. Baumjohann, *Advanced Space Plasma Physics* (Imperial C.P., London, 1997).
[4]D. Tskhakaya, "The particle-in-cell method," in *Computational Many-Particle Physics*, edited by H. Fehske, R. Schneider, and A. Weiße (Springer Berlin Heidelberg, Berlin, Heidelberg, 2008), pp. 161–189.
[5]J. M. Dawson, "Particle simulation of plasmas," Rev. Mod. Phys. **55**, 403–447 (1983).
[6]R. W. Hockney and J. W. Eastwood, *Computer Simulation Using Particles* (Hilger, Bristol, 1988).
[7]I. Hutchinson, "How can slow plasma electron holes exist?," Phys. Rev. E **104**, 015208 (2021).
[8]R. S. Rajawat and S. Sengupta, "Particle-in-cell simulation of Buneman instability beyond quasilinear saturation," Phys. Plasmas **24**, 122103 (2017).
[9]E. Koen, A. Collier, S. Maharaj, and M. Hellberg, "Particle-in-cell simulations of ion-acoustic waves with application to Saturn's magnetosphere," Phys. Plasmas **21**, 072122 (2014).
[10]UCLA, "Jupyter notebooks for educational plasma physics simulations with PIC," <https://github.com/UCLA-Plasma-Simulation-Group/JupyterPIC>.
[11]Y. Omura and H. Matsumoto, *KEMPO1: Technical Guide to One-Dimensional Electromagnetic Particle Code* (Terra Scientific, Tokyo, 1993).
[12]D. Rodríguez-Patiño, S. Ramírez Ramírez, J. Hoyos, J. Salcedo Gallo, and E. Restrepo Parra, "Implementation of the two-dimensional electrostatic particle-in-cell method implementation of the two-dimensional electrostatic particle-in-cell method," Am. J. Phys. **88**, 159–167 (2020).
[13]G. Lapenta, "Particle-in-cell 1D electrostatic code," (2007), <https://github.com/valsusa/SkeletonPIC>.
[14]S. Gomez, J. H. Hoyos, and J. A. Valdivia, "PlasmAPP code," (2022), <https://github.com/gsara798/PLASMAPP-0.1.git>.
[15]See supplementary material at https://www.scitation.org/doi/suppl/10.1119/5.0135515 for *PlasmAPP code* and supplementary notes.
[16]F. Reif, *Fundamentals of Statistical and Thermal Physics* (McGraw Hill, Tokyo, 1965).
[17]G. Lapenta, "Kinetic plasma simulation: Particle in cell method," in *Proceedings of the XII Carolus Magnus Summer School on Plasma and Fusion Energy Physics* (KU Leuven, Belgium, 2015).
[18]S. Ledvina, Y. Ma, and E. Kallio, "Modeling and simulating flowing plasmas and related phenomena," Space Sci. Rev. **139**, 143–189 (2008).
[19]R. Goldston and P. H. Rutherford, *Introduction to Plasma Physics* (CRC Press, Boca Raton, FL, 2020).
[20]J. A. Bittencourt, *Fundamentals of Plasma Physics*, 3rd ed. (Springer-Verlag, New York, 2004).
[21]P. M. Bellan, *Fundamentals of Plasma Physics* (Cambridge U. P., Cambridge, 2006).
[22]N. Krall, A. Trivelpiece, and J. Kempton, *Principles of Plasma Physics*, International Series in Pure and Applied Physics (McGraw-Hill, New York, 1973).
[23]K. Chaudhary, A. M. Imam, S. Z. H. Rizvi, and J. Ali, in *Kinetic Theory*, edited by G. Z. Kyzas and A. C. Mitropoulos (IntechOpen, Rijeka, 2018), Chap. 7.
[24]H. Ruhl and P. Mulser, "Relativistic Vlasov simulation of intense fs laser pulse-matter interaction," Phys. Lett. A **205**, 388–392 (1995).
[25]A. Pukhov, "Particle-in-cell codes for plasma-based particle acceleration," *Proceedings of the 2014 CAS-CERN Accelerator School: Plasma Wake Acceleration, 23–29 November 2014, Geneva, Switzerland* (CERN, Geneva, 2016), pp. 181–206.
[26]R. E. Navarro, P. S. Moya, V. Muñoz, J. A. Araneda, A. F. Viñas, and J. A. Valdivia, *Solar Wind Thermally Induced Magnetic Fluctuations*, Vol. 112 (American Physical Society, College Park, Maryland, 2014), p. 245001.
[27]V. Sainia, S. K. Pandey, P. Trivedi, and R. Ganesh, "Coherent phase space structures in a 1D electrostatic plasma using particle-in-cell and Vlasov simulations: A comparative study," Phys. Plasmas **25**, 092107 (2018).
[28]S. K. Pandey and R. Ganesh, "Landau damping in one dimensional periodic inhomogeneous collisionless plasmas," AIP Adv. **11**, 025229 (2021).
[29]R. L. Burden and J. D. Faires, "Numerical analysis," 4th ed., *The Prindle, Weber and Schmidt Series in Mathematics* (PWS-Kent Publishing Company, Boston, 1989).

[30]J. S. Blandón, J. P. Grisales, and H. Riascos, *Electrostatic Plasma Simulation by Particle-In-Cell Method Using ANACONDA Package*, Vol. 850 (IOP Publishing, Bristol, 2017), p. 012007.
[31]I. Hutchinson, "Electron holes in phase space: What they are and why they matter," Phys. Plasmas **24**, 055601 (2017).
[32]F. F. Chen, *Introduction to Plasma Physics* (Plenum Press, New York, 1974).
[33]F. Gbaorun, E. S. John, T. M. Aper, T. Daniel, and F. Eriba-Idoko, "Simulation of electron-electron two stream instability (ETSI)," Nigerian Annals of Pure and Applied Sciences **2**, 265–273 (2019).
[34]G. Lapenta, "Particle simulations of space weather," Comput. Plasma Phys. **231**, 795–821 (2012).
[35]J. S. Pickett, L.-J. Chen, S. W. Kahler, O. Santolík, M. L. Goldstein, B. Lavraud, P. M. E. Décréau, R. Kessel, E. Lucek, G. S. Lakhina, B. T. Tsurutani, D. A. Gurnett, N. Cornilleau-Wehrlin, A. Fazakerley, H. Rème, and A. Balogh, "On the generation of solitary waves observed by cluster in the near-Earth magnetosheath," Nonlin. Processes Geophys. **12**, 181–193 (2005).
[36]MATLAB, *Create Codistributed Array of Normally Distributed Random Numbers*, <https://la.mathworks.com/help/parallel-computing/codistributed.randn.html>.
[37]Numpy. "Return a sample (or samples) from the 'standard normal' distribution," <https://numpy.org/doc/stable/reference/random/generated/numpy.random.randn.html>.
[38]H. E. J. Koskinen, *Physics of Space Storms from the Solar Surface the Earth* (Springer, Berlin, 2011).
[39]Q. Moreno, M. E. Dieckmann, X. Ribeyre, S. Jequier, V. T. Tikhonchuk, and E. d'Humières, "Impact of the electron to ion mass ratio on unstable systems in particle-in-cell simulations," Phys. Plasmas **25**, 062125 (2018).
[40]M. V. Goldman, D. L. Newman, and R. E. Ergun, "Phase-space holes due to electron and ion beams accelerated by a current-driven potential ramp," Nonlin. Processes Geophys. **10**, 37–44 (2003).

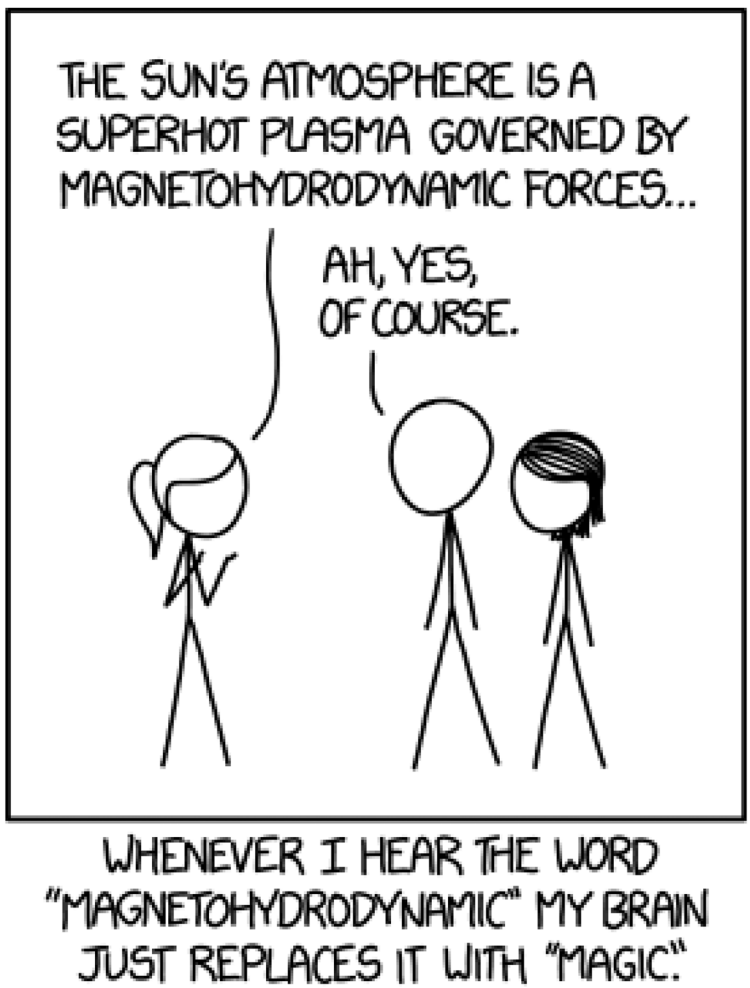

"Magnetohydrodynamics combines the intuitive nature of Maxwell's equations with the easy solvability of the Navier-Stokes equations. It's so straightforward physicists add "relativistic" or "quantum" just to keep it from getting boring." (Source: https://xkcd.com/1851/)